Fusion of Texture Measures for Urban Area Characterization

Giovanna Trianni, Marika Tosi, Fabio Dell'Acqua, Paolo Gamba
Department of Electronics, University of Pavia
Via Ferrata, 1
27100 Pavia
Italy
paolo.gamba@unipv.it

Abstract – *This paper shows an application of textural features for urban area characterization using SAR satellite images. The proposed method is based on the use of a fuzzy ARTMAP classifier whose input is selected, among many possible texture measures, by means of the Histogram Distance Index (HDI).*

Results validate the choice of HDI as a feature selection index. Moreover, they show that the joint use of multiple, complementary information about the spatial neighborhood of each pixel helps in delineating some land use classes that are usually considered unresolvable in satellite SAR images.

Keywords: SAR, co-occurrence matrix, image fusion, urban remote sensing.

1 Introduction

This work has been developed in the framework of urban remote sensing and data fusion, which is one of the most promising applications of satellite and airborne sensor data. As a matter of fact, environmental monitoring of urban areas seems to be one of the main requests by the citizens around the world. In Europe the Global Monitoring for Environment and Security initiative (GMES) recognizes this need and addresses this topic by means of an industrial project aimed at producing GMES urban services (GUS, [1]). In USA many projects are considering urban remote sensing (e. g. [2]) as a result of homeland security programs and/or a renewed interest in environment-aware urban planning.

Although urban remote sensing is generally assumed as a sector of remote sensing strictly related to very high resolution (VHR) sensors, even relatively coarse resolution images may be helpful in a number of ways. There are issues like global warming or energy exchange among land, ocean and atmosphere that have in urban areas their focal points [3], but need a global view to understand their dynamics. There are also requests of urban-related information, especially soil sealing, at a regional level [4]. Finally, there are disaster management systems relying on remote sensing data and aimed at monitoring the areas where the majority of the world's population lives, i. e. towns and cities. In summary, even if less known than for VHR imagery, there is a widespread interest for satellite information at a scale allowing a less accurate land cover characterization from the point of view of the single residential built up structure. These information, however, are extremely useful for all the above mentioned fields of work.

Among the satellite sensors providing such kind of data, the synthetic aperture radar (SAR) is well suited for its all-weather capabilities, but suffers, in urban areas, for its side-looking nature. Moreover, there are plans by many space agencies (the German and Italian ones, for instance) to launch satellites with high resolution SAR sensors in the near future. This, in turn, will provide a huge amount of radar data to be processed in urban areas for environmental and security purposes. So, SAR data exploitation at a commercial level for some kind of urban planning, management or monitoring is a currently pursued research & development (R&S) field [5].

The paper is structured as follows: section II reviews, even if very briefly, current trends in image fusion of remote sensing data with respect to urban remote sensing applications. Section III introduces the processing chain we have proposed and implemented, while the following section is devoted to present our test data set and the experimental results. The final section provides some comments and a discussion about the achievements of this work, as well as some ideas for the future.

2 Fusion of spectral and spatial information in urban remote sensing

As stated in the introduction, no data set or sensor alone is able to capture the variability of an urban environment. So, urban data fusion has been increasingly considered in the past years. In particular, recent workshops [6, 7] showed that there is a remarkable interest in using complex and Interferometric SAR data for different urban applications, from mapping to building extraction to subsidence monitoring. Despite all the problems coming from its above mentioned side-looking nature, radar deserves some more attention for its potentials in this area, especially considering the availability in the near future of high resolution data coming from TerraSAR-X [8] or Cosmo/SkyMed [9] low orbit satellites. This calls also for advanced SAR simulators suited for urban areas [10], and systematic evaluation of the best geometrical (position, look angle) and electromagnetic (frequency, bandwidth, polarization) configuration for the radar system [11]. Unfortunately, such analyses can not be

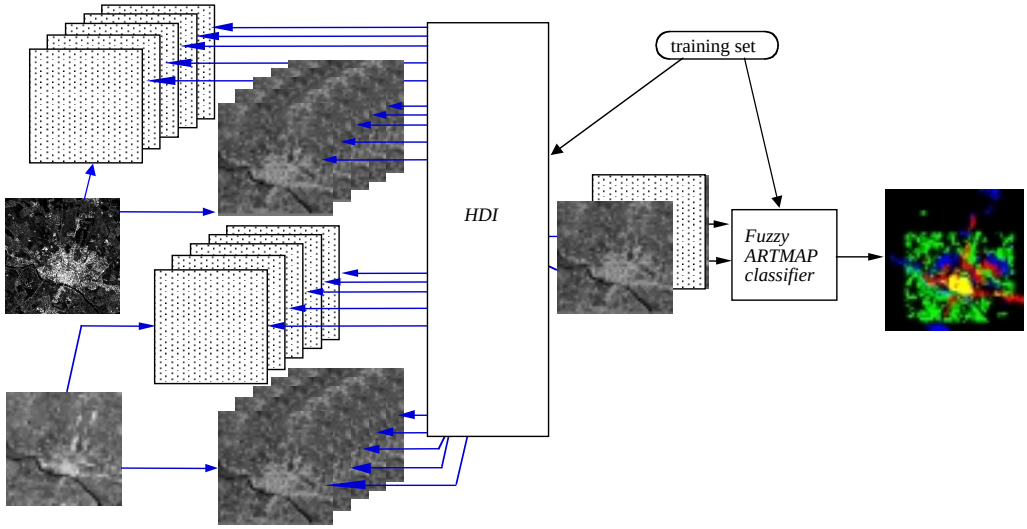

Fig. 1: Conceptual workflow of the proposed multi-scale and multi-temporal combination of textural features using HDI and fuzzy ARTMAP.

found in classic SAR image processing and interpretation textbook, like for instance [12]

A second, extremely interesting topic in urban data fusion is related to the fusion of panchromatic and multispectral data from satellite sensors [13], with the aim to provide as much as possible "the best of the two worlds", i. e. high resolution multispectral data. The need for such a tool for urban area characterization is of course very urgent, and current methods are now passing from the theoretical to the implementation stage [14, 15].

Moreover, we have to stress the increasing importance of interpretation techniques well suited for very high resolution data [16], which means techniques very similar to those already in use for aerial images, but with the advantages of reduced revisit time (so, better monitoring capabilities) and more bands (better land cover discrimination). Still, it is questionable at this moment if we will be able to reduce problems in coregistration and vertical and horizontal accuracy [17], and this will be one of the open questions in the future, mainly requiring data fusion issues at a feature level for a better overall result.

Finally, it's important to note that there is a large literature trying to exploit spatial as well as spectral information in urban areas. Examples are new classification techniques [18] based on morphological profiles for a better understanding of the scene, statistical analysis for enhanced segmentation of urban environments [19], and texture analysis of urban areas to describe spatial features useful for further characterizations [20]. Within this group we must consider also papers coming from the image fusion community, such as [21], whose approach is in some respect very similar to the one independently proposed in this paper and in related ones. It employs spatial as well as spectral features to extract information about specific targets or land cover classes using a neuro-fuzzy classifier after choosing the best feature set using the internal representation of the same classifier. A different, but equally interesting approach, based on Multi-Perceptron neural networks has been proposed in [22]. Here the authors assume as input to the first layer of the network the output of many spatially different filters, and let the network choose the weights of the input to hidden nodes connections. They define the relative importance of each filter output for the classification/segmentation problem described by means of the training set.

3 Fusion of multi-scale textural feature

This work refers to the analysis of multi-temporal/multiple sensors' SAR imagery for the recognition of different classes inside an urban area. Note that these classes are not comparable with those that we may extract from finer spatial resolution data. In particular, we can't rely on the analysis of the building aggregation, because of the coarse resolution. Our results show, however, that satellite SAR images are a source of information sufficient to segment urban scenes into the most relevant structures at the block scale.

The starting point is a set of input bands, derived by a spatial analysis of the SAR images under test. We have proved [20] that co-occurrence measures are useful for ur-

ban characterization using satellite SAR images. Unfortunately, there are multiple parameters that must be chosen: the subset of measures, the width of the co-occurrence window, and the displacement used to compute the co-occurrences. These parameters may change from image to image, even for the same classification problem, because the statistical properties of SAR images are strongly dependent from the looking direction, the radar frequency, bandwidth and pulse repetition frequency (PRF). Moreover, if we have more images, we have to consider even larger data sets. So, the main problem becomes how to choose "on the fly" the best input subset for a classification problem. In other words, we need to define a strategy to fuse the information about spatial aggregation of pixels in the input image set, being able to choose the information sources best suited for a given task.

Our choice, unlike in [21], is to separate the information selection step from the information fusion. Of course, we need to rely on tools well integrated, but the processing chain is split in two steps, as presented graphically in Fig. 1.

1. The first step is, as recalled before, essentially a feature selection step. The training samples define a specific classification (or segmentation) problem. In our situation, for example, the problem is the extraction of three urban land use classes and the consequent segmentation of one or more SAR images into these classes, plus vegetation and open water (see next section for details). For this task, some of the input bands may be more useful than others.

   For classification purposes, the usual way to reduce the input order is to verify the separability of the classes we are looking for, and pick the input subset where separability is maximum. The question therefore is: which the best separability tool to use? We suggest to consider the Histogram Distance Index (HDI [23]), better correlated than other indexes with the tool exploited in the second step of this procedure.

2. The second step is indeed a classification step, and the tool we use is a neuro-fuzzy chain based on fuzzy ARTMAP neural networks [24]. Adaptive Resonance Theory (ART) networks, basically introduced for solving pattern recognition problems, have indeed shown to be very efficient in multi-band remote sensing data analysis. This is particularly true when we deal with bands whose statistical properties are very different, as is the case with texture measures. ART networks store in their memories information about the training samples, and compare test patterns with these memories. Any match assigns the pattern to an output category, e. g. a land use class.

In the fuzzy ARTMAP structure, the above mentioned memories are stored in the *category layer* and updated using a fuzzy AND operator using new training patterns. The fuzzy operator is essential a band-by-band *min* operator among the values of the training patterns, and translates the (normalized) input into a suitable internal set of ranges. Each range set delimits a *hypercube*, and one or more hypercubes are connected to a given output class. In a sense, the fuzzy ARTMP training phase builds a "decision tree" internal to the fuzzy ARTMAP structure, that provides a set of rules for the assignment of a new, unknown pattern to one of the known classes. The parameters of the ART networks rule this mechanism, and determine the number and shape of these hypercubes. They act as regularization factors in the segmentation of the hyperspace which is the internal data representation of the neural network, and as resilience factors, determining how long a training input is going to influence a network memory.

Independently from the choice of these parameters, the training patterns are mapped into an internal **finite** hyperspace, because of the normalization step which is the first one in any ART network structure. This means that a statistical representation of the memory patterns does not fit into the most widely used for remote sensing data, i. e. the normal (or log-normal) distribution. So, if we want to determine which are the best suitable input bands for a given training set, we can't reasonably rely on separability indexes based on this assumption. At least, we should consider different ways to map separability, based on **finite dimension hyperspaces**.

Our experience shows that a good candidate for this task is the already mentioned HDI, whose definition is :

$$\text{HDI} = \sum_{i,j} \left(\frac{1 - 2 \sum_{TS_{ij}} \min\left(f_i(\vec{x}), f_j(\vec{x})\right)}{\sum_{TS_{ij}} \left(f_i(\vec{x}) + f_j(\vec{x})\right)} \right) \quad (1)$$

where $\vec{x}$ is the generic multi-band pixel, i. e. the vector of band values, and $f(\vec{x})$ represents the histogram (or non-normalized probability density function) of $\vec{x}$. More precisely, HDI is computed by summing the separability between class i and class j, for each possible class pair in the training set. In turn, each term is computed by considering the separability of the histograms $f_i(\vec{x})$ and $f_j(\vec{x})$, computed by considering the subset of the total training set referring to classes i and j, TS_{ij}. Finally, the histogram separability is computed by quantifying the overlapping between $f_i(\vec{x})$ and $f_j(\vec{x})$.

In the end, HDI may be considered as the mean of the separability between any possible couple of classes in the training set. It is built on the histogram function $f(\vec{x})$, which is actually a map of the clusters of the multidimensional training samples in the multidimensional feature space. In other words, HDI computes how much the cluster of training samples referring to two different classes overlap, but without assuming a precise model for the probability density function. Therefore, no assumption outside of the range of values in the training set is done.

To provide a reference and compare experimentally HDI performances, we recall here the definition of the well-known Transformed Divergence Index (TD) and Jeffrey-Matsushita Index (J-M), [25]:

$$\begin{aligned} D_{ij} &= \frac{1}{2}\, trace\left[\left(\mathbf{V}_i - \mathbf{V}_j\right)\left(\mathbf{V}_j^{-1} - \mathbf{V}_i^{-1}\right)\right] \quad (2) \\ &+ \frac{1}{2}\, trace\left[\left(\mathbf{V}_i^{-1} + \mathbf{V}_j^{-1}\right)\left(\mathbf{m}_i - \mathbf{m}_j\right)\left(\mathbf{m}_i - \mathbf{m}_j\right)^T\right] \end{aligned}$$

$$\text{TD} = \sum_{i,j} 2\left(1 - e^{-\frac{D_{ij}}{8}}\right) \quad (3)$$

$$B_{ij} = \frac{1}{8}\left(\mathbf{m}_i - \mathbf{m}_j\right)^T \left[\frac{\mathbf{V}_i + \mathbf{V}_j}{2}\right]^{-1} \left(\mathbf{m}_i - \mathbf{m}_j\right) + \frac{1}{2}\log \frac{\left|\frac{\mathbf{V}_i + \mathbf{V}_j}{2}\right|}{\sqrt{|\mathbf{V}_i||\mathbf{V}_j|}} \quad (4)$$

$$\text{J-M} = \sum_{i,j} \sqrt{2}\left(1 - e^{-B_{ij}}\right) \quad (5)$$

where $\mathbf{m}_i = E(\vec{x})$, and the expected value $E(\cdot)$ is computed on the subset of the training set belonging to class i. Similarly, $\mathbf{V}_i$ is the variance/covariance matrix of $\vec{x}$. Of course, these definitions implicitly call for normal probability functions, since they assume that the mean and the variance are enough to characterize the statistical behavior of the training set.

Note that HDI varies between 0 and 1 as a function of the superposition of the histograms. The more a texture measure is useful to discriminate between two classes, the more its corresponding distributions (represented by $f_i(x)$ and $f_j(x)$) are different, and the higher the HDI value. Similarly for TD and JM, although their range is between 0 and 2.

If we compare the results of these three indexes we don't find, of course, the same results, because of the different *a priori* assumptions about the $f_i(x)$ distributions. More precisely, it is very unlikely that TD and J-M assume their bottom or top values, because the normal distribution have infinite support, and there is always some degree of overlap, very small but never null. On the contrary, HDI may assume very easily the value 1, when the finite range of the training samples define for all the classes nonoverlapping clusters in the input multidimensional space. If we assume that the training samples are representative of the classes they belong to, we can use this information to define how many features are "enough" for a given classification task. With the other indexes, we would never be able to limit the number of input bands, unless we put a threshold on the difference between their value and the top of their range. With HDI we are lead to a natural definition of the input set which is both *necessary and sufficient* for a given task. Moreover, HDI respects the finite support of the $f_i(x)$ distributions. We have shown that the input range is translated into the memories of the fuzzy ARTMAP neural network classifier but maintains its finite support. So, we may expect that the separability computed by means of HDI holds in both the original input space and the internal memory space. We will prove experimentally this assumption by comparing the values of the three indexes on the same set and correlating them with the actual classification results after the second step of our procedure.

We would like to add a final comment. We want to stress that the common feature among our approach, [21] and [22] is the ability to choose in a dynamic manner the inputs and exploit the usefulness of each new spatial/spectral band. The difference is clear if we compare these methodologies with those presented for instance in [26], where many fixed schemes of textural bands are compared and the best one is provided, after an exhaustive but static analysis has been performed.

4 Experimental results

The above mentioned procedure were applied using a sufficiently large data base of SAR images over the same urban area. The set was collected because of the research in urban remote sensing carried by the Department of Electronics of the University of Pavia.

4.1 Image test set

The image data set contains many different SAR amplitude images, referring to the urban test area of Pavia, Northern Italy. The most recent images were recorded in 2002 and in 2003 by the ASAR sensor on board of the ENVISAT satellite. They are two ascending and one descending image, resampled from single look, slant range complex data. We have single polarization or alternate polarizations. Therefore, we may understand the role of different backscattering effects in urban areas. The less recent images come from the SAR sensor on board of the ERS-1/2 satellites. They refer to almost 10 years of observations, from August 1992 to October 2000. The total is 9 images, mostly descending. Finally, we have RADARSAT-1 data recorded between October 2000 and September 2001. They refer to multiple viewing angles, and in some cases to a finer spatial resolution.

For the purpose of data analysis, a ground truth was built by visual interpretation of very fine resolution optical satellite images on the same area, together with the corresponding sector of the Technical Regional Map. This double check was needed because the SAR data cover more than 10 years of temporal range, and the map is based on aerial data recorded around 1990, while the fine resolution satellite data refers to July 2001. Since the data sets from ERS and ENVISAT have different spatial resolution than the RADARSAT-1 images, two copies of the same ground truth were provided, at 12.5 m and 7 m ground resolution, and all the SAR data, possibly after a slant to ground-range conversion, were coregistered to one of these two reference maps. The training set was based on a small subset of the ground truth maps, suitably chosen, and the same training set is used for texture comparison, as explained in Section 2.

A sample of the area of interest in a RADARSAT-1 fine beam mode is shown in Fig. 2(a), while fig. 2(b) is the corresponding ground truth. Vegetation is depicted in green, water in light blue, the city center in yellow, the residential areas in red and, finally, the suburban zones in blue.

As already described, our procedure is aimed at using textural features extracted from the co-occurrence matrix: the width of the window used to compute these features is the first and maybe most important parameter to be chosen, Of course, some kind of *a priori* knowledge on the scene may help. For instance, we have found in [20] that a good choice is the mean block size in the urban area of interest.

Table 1: Confusion Matrix for the classification maps in Fig. 4 (details in the text)

Fig. 4(a)	Center	Residential	Suburban	Water	Vegetation	*Omis. acc.*
Center	10476	16413	6546	78	1940	29.6%
Residential	3611	16291	39033	1595	15175	21.6%
Suburban	2842	11188	32247	4739	24906	42.5%
Water	7	51	930	5594	3646	54.7%
Vegetation	277	3186	22787	1678	196701	87.6%
Comm. acc.	60.9%	34.6%	31.8%	40.9%	81.2%	OA = 61.9%

Fig. 4(b)	Center	Residential	Suburban	Water	Vegetation	*Omis. acc.*
Center	8137	6373	1170	25	40	51.7%
Residential	2773	19919	9551	539	899	59.1%
Suburban	280	10792	14404	3007	5233	42.7%
Water	0	150	1137	1104	2136	24.4%
Vegetation	115	4120	14900	8896	71773	71.9%
Comm. acc.	72.0%	48.2%	35.0%	8.1%	89.6%	OA = 61.5%

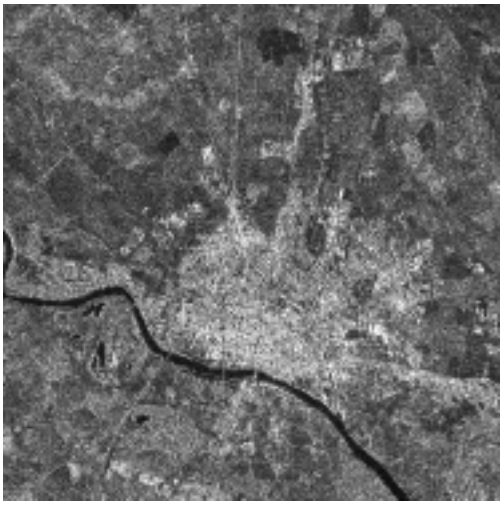

(a)

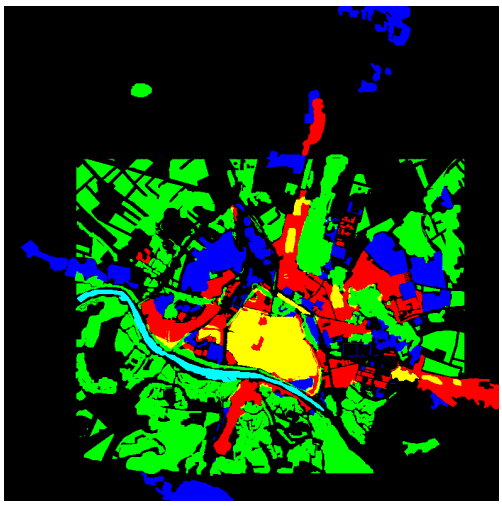

(b)

Fig. 2: (a) A sample SAR image of the urban test area of Pavia, Northern Italy (RADARSAT-1 fine beam mode); (b) the corresponding ground truth (colors are discussed in the text).

More generally speaking, however, this information is not known or, at least, not sufficiently clear. We may guess a range of values, but it is difficult to be sure about a single number. The second choice is about the textural features that we need, how many of them and which ones. Even in this case we may have some knowledge of the subset which is the best for a given image, but differences in SAR images referring to the same scenes are huge, and correlation (or, better, de-correlation) in amplitude images between different passages of the same sensor with even the same looking angle are small but still exists. Moreover, as in our image set, different looking angles or ascending and descending modes may be considered, and different subset might be chosen. Finally, different spatial ground resolution reveal different details, introducing complexity but also different textural features in the same scene, that were invisible and therefore useless, for instance, in coarser resolution images.

So, there are many different problems that we may face in analyzing our test set, and two of them are here considered in detail, in order to discuss our procedure and highlight its advantages and discover problematic points.

4.2 Combination of textural features at a given scale

The first example we want to discuss is the definition of the "best" texture set for a given problem. To this aim, as explained in the previous section, we use HDI, and compare results with the other two indexes, TD and J-M. For our experiments, we consider the image in Fig. 2(a), recorded by the RADARSAT-1 satellite in fine beam mode, with 40° looking angle, VV polarization.

We assume that the width dimension used in [20] and referring to the mean block size in the test area i still valid. In that paper we used a 21×21 pixel window in co-occurrence computation, with a ground spatial resolution of nearly 10.5 m. This choice translates into a 31×31 window for the current image, at a finer spatial resolution. After computing eight co-occurrence features (mean, variance, homogeneity, correlation, dissimilarity, entropy, contrast and second moment), a first computation of the HDI, TD and J-M values for any possible combination shows that very high values

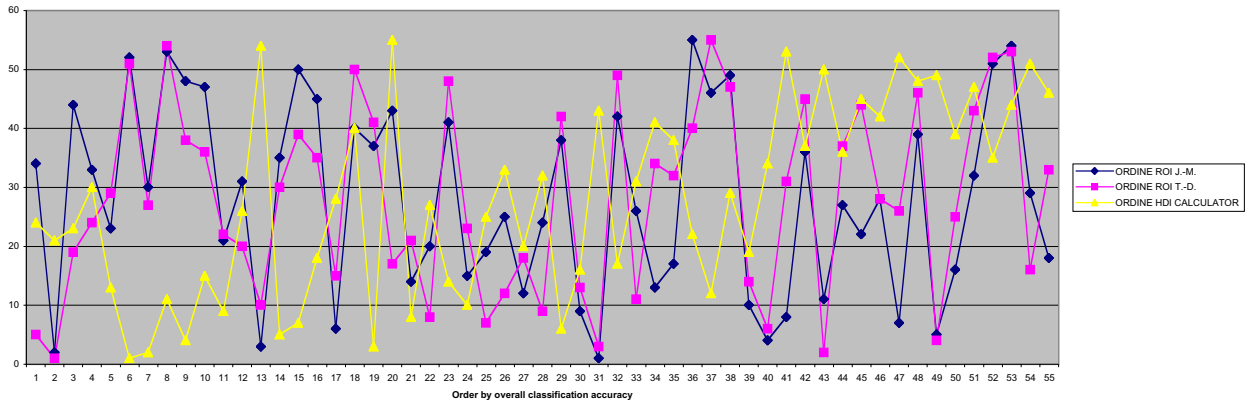

Fig. 3: The ordered position of each possible combination of three texture measures (out of eight, see text) for the RADARSAT-1 image in Fig. 2(a), in terms of J-M, TD and HDI values, respectively. The *x*-axis defines the order based on classification accuracy.

of these indexes are already found using subsets of just two or three texture measures. So, in the following we explore, for sake of simplicity, all the possible combinations of no more than three features. We compare the order of these combination using any of these three indexes with the order found experimentally by classifying the same combination using the fuzzy ARTMAP classifier.

Fig. 3 shows the comparison. The *x*-axis defines the order based on increasing classification accuracy. We note that there is almost no correlation between the classification results determining the order on the *x*-axis and the order coming from J-M or TD values (related with the *y*-axis). On the contrary, HDI-based order is sufficiently similar to have a correlation index around 0.6. The best classification map is shown in Fig. 4(a), while the confusion matrix is shown in Table 1. There are a few differences on the behavior of the ground truth classes. As a matter of fact, the finer spatial resolution of the RADARSAT SAR allows a better understanding of the urban center, which the ground truth, originally designed for ERS and ENVISAT data, represents in a too coarse manner. Moreover, we have a larger mixture of the urban classes than in ERS-derived classifications, perhaps for the same reason. The structure of the urban area is however well delineated and clearly discriminated from the agricultural surround.

4.3 Combination of multi-scale features for a given texture set

The second example takes into account the uncertainty on the scale of the objects in the image, and therefore in the width of the co-occurrence window. In particular, we want to explore if the use of different window width for a given texture subset is able to provide a better classification map that the same combination with all the features referring to the same scale. To this aim, we use the Alternate Polarization (AP) image recorded by the ASAR sensor using the HH/VV polarizations on August 29^{th}, 2003. We arbitrarily consider a subset of two very simple features: mean and variance.

Choosing among four different widths (19, 21, 23 and 25 pixels) instead of using a fixed neighborhood, we find that different scale combinations provide the largest overall accuracy for for the two polarizations. In particular, HDI analysis recommends using 21 and 25 pixels for the two above mentioned measures using HH polarization, and 19 pixels for both using VV polarization. The corresponding "best" classification maps are shown in fig. 4(b) and (c) for HH and VV polarization, respectively. The confusion matrix for the first situation is shown again in Table 1. A first comment is that the second polarization does not allow a sufficient recognition of the land cover classes outside the urban area. Both polarization show, instead, a similar behavior for urban land covers. Even in this case we do not find very large omission and commission accuracy for the urban classes, but the classification pattern is very similar for both polarizations.

5 Conclusions

This paper discusses a methodology to fuse textural information extracted from SAR images for a better classification of urban environments. The results validate the choice of the HDI/Fuzzy ARTMAP chain for feature selection/classification. In particular, we have found that

- HDI is intimately correlated with the internal Fuzzy ARTMAP feature space, and there is a sufficient correlation between the overall accuracy after classification and the HDI values;
- HDI can be used to define the best feature set for a given classification problem; the extraction of urban land cover classes using texture measures can be suitably addressed using this tool;
- for a given combination of co-occurrence texture measure it may be better to use different window widths, chosen again by means of the HDI feature reduction step.

These are the major achievements of this paper, and the original results of this research. Of course, the approach still needs to be validated in some ways, for insatnce by considering more urban areas. Moreover, we have to investigate the possible strong dependence of radar backscatter from the viewing angle. The results we have with ERS

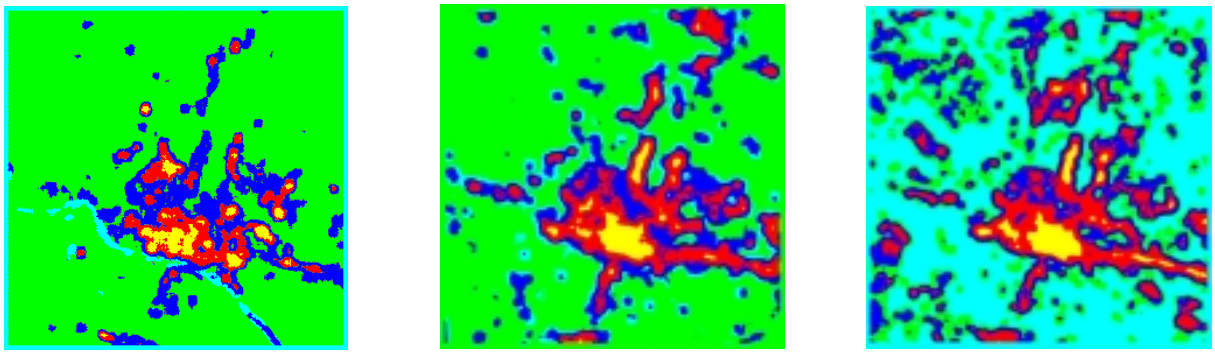

(a) (b) (c)

Fig. 4: The classification maps for (a) the best classification of three textural features for the RADARSAT image in Fig. 2(a) and (b,c) the best classification results of mean and variance each one computed with a suitable co-occurrence window width (ASAR AP image, HH and VV polarizations, respectively).

and RADARSAT data are sufficiently different to call for a deeper analysis. Moreover, we need to consider different polarizations and possibly combine them considering the same texture from different images or different textures from different images. Finally, it is possible to investigate temporal texture measures together with spatial ones, even if this will increase the complexity of the problem.

Acknowledgements

The authors wish to thank Gianluca Pulina for developing and maintaining the fuzzy ARTMAP and HDI software.

References

[1] GUS home page: http://www.gmesurbanservices.com

[2] Urban Environmental Monitoring (UEM) Project - Global Urban Monitoring with ASTER, project home page at Arizona State University: http://elwood.la.asu.edu/grsl/UEM/

[3] C. Lavalle, L. Demicheli, M. Kasanko, N. McCormick, J. Barredo, M. Turchini, M. da Gra Saraiva, F. Nunes da Silva, I. Loupa Ramos, F. Pinto Monteiro, M. Caetano. Towards an urban atlas: Assessment of spatial data on 25 European cities and urban areas. Environmental issue report No 30, European Environmental Agency, Copenhagen, 2002.

[4] N. McCormick, C. Lavalle, M. Kasanko, L. Demicheli, J. Barredo. Mapping and modelling the impact of land use planning and management practices on urban and peri-urban landscapes in Europe: the MOLAND project. In *Proc.* 2^{nd} *GRSS/ISPRS Joint Workshop on "Remote Sensing and Data Fusion over Urban Areas"*, pages 242-243, Berlin, Germany, 22-23 May 2003. IEEE, Piscataway, NJ, 2003.

[5] C.Boehm, R.Schenkel. Analysis of High Resolution Polarimetric SAR in Urban Areas. In *Proc. of the Workshop on workshop on Advances in Techniques for Analysis of Remotely Sensed Data*, 27-28 October 2003, Greenbelt (MD). IEEE, Piscataway, NJ, 2003.

[6] *Proc.* 1^{st} *IEEE/ISPRS Joint Workshop on "Remote Sensing and Data Fusion over Urban Areas"*, Rome, Italy, 8-9 November 2001. IEEE, Piscataway, NJ, 2001.

[7] *Proc.* 2^{nd} *GRSS/ISPRS Joint Workshop on "Remote Sensing and Data Fusion over Urban Areas"*, Berlin, Germany, 22-23 May 2003. IEEE, Piscataway, NJ, 2003.

[8] A. Roth. TerraSAR-X: A new perspective for scientific use of high resolution spaceborne SAR data. In *Proc.* 2^{nd} *GRSS/ISPRS Joint Workshop on "Remote Sensing and Data Fusion over Urban Areas"*, pages 4-8, Berlin, Germany, 22-23 May 2003. IEEE, Piscataway, NJ, 2003.

[9] F. Caltagirone, p. Spera, R. Vigliotti, G. Manoni. SkyMed/COSMO mission overview. In *Proc. of the IEEE Int. Geoscience and Remote Sensing Symposium Proceedings, 1998*, Vol. 2, pages 683 -685, Seattle (WA), 6-10 July 1998. IEEE, Piscataway, NJ, 1998.

[10] G. Franceschetti, A. Iodice, D. Riccio, G. Ruello. Information content in SAR images of urban areas. In *Proc.* 2^{nd} *GRSS/ISPRS Joint Workshop on "Remote Sensing and Data Fusion over Urban Areas"*, pages 42-45, Berlin, Germany, 22-23 May 2003. IEEE, Piscataway, NJ, 2003.

[11] U. Soergel, U. Thoennessen, U. Stilla. Visibility analysis of man-made objects in SAR images. In *Proc.* 2^{nd} *GRSS/ISPRS Joint Workshop on "Remote Sensing and Data Fusion over Urban Areas"*, pages 119-123, Berlin, Germany, 22-23 May 2003. IEEE, Piscataway, NJ, 2003.

[12] S. Quegan, C. Oliver, *Understanding SAR images"*, Artech House, Boston, 1998.

[13] A. Garzelli, B. Aiazzi, L. Alparone. S. Baronti. An MTF-Based Spectral Distortion Minimizing Model for Pan-Sharpening of Very High Resolution Multispectral Images of Urban Areas. In *Proc.* 2^{nd} *GRSS/ISPRS Joint Workshop on "Remote Sensing and Data Fusion over Urban Areas"*, pages 89-93, Berlin, Germany, 22-23 May 2003. IEEE, Piscataway, NJ, 2003.

[14] C. Latry. H. Vadon, M.-J. Lefevre, H. de Boissezon. SPOT5 THX : a 2.5m fused product. In *Proc.* 2^{nd} *GRSS/ISPRS Joint Workshop on "Remote Sensing and Data Fusion over Urban Areas"*, pages 86-88, Berlin, Germany, 22-23 May 2003. IEEE, Piscataway, NJ, 2003.

[15] F. Laporterie, C. Latry, H. De Boissezon, M-J. Lefvre. Evaluation of the quality of panchromatic / multispectral fusion algorithms performed on images simulating the future

Pleiades satellites. In *Proc. 2^{nd} GRSS/ISPRS Joint Workshop on "Remote Sensing and Data Fusion over Urban Areas"*, pages 94-97, Berlin, Germany, 22-23 May 2003. IEEE, Piscataway, NJ, 2003.

[16] J.A. Benediktsson, K. Arnason, M. Pesaresi. Morphological profiles used for classification of data from urban areas. In *Proc. of the IEEE Int. Geoscience and Remote Sensing Symposium, 2002*, Vol. 1, pages 305-307, Toronto, Canada, 24-28 June 2002. IEEE, Piscataway, NJ, 2002.

[17] C.H. Davis and X. Wang. Planimetric accuracy of Ikonos 1 m panchromatic orthoimage products and their utility for local government GIS basemap applications. *Int. J. Remote Sensing*, 24(22): 42674288, 2003.

[18] J.A. Benediktsson, M. Pesaresi,K. Arnason. Classification and feature extraction for remote sensing images from urban areas based on morphological transformations. *IEEE Trans. on Geoscience and Remote Sensing*, 41(9): 1940-1949, 2003.

[19] T. Macr Pellizzeri, M. Sciotti, P. Lombardo, M. Meloni. Model-based processing of multifrequency polarimetric SAR images of urban areas. In *Proc. 2^{nd} GRSS/ISPRS Joint Workshop on "Remote Sensing and Data Fusion over Urban Areas"*, pages 46-51, Berlin, Germany, 22-23 May 2003. IEEE, Piscataway, NJ, 2003.

[20] F. Dell'Acqua, P. Gamba. Texture-based characterization of urban environments on satellite SAR images- *IEEE Trans. on Geoscience and Remote Sensing*, 41(11): 153-159, 2003.

[21] W.W. Streilein, A. Waxman, W.D. Ross, F. Liu, M. Braun, D. Fay, P. Harmon, and C.H. Read. Fused Multi-Sensor Image Mining for Feature Foundation Data. In *Proc. of the 3^{rd} Int. Conf. Information Fusion*, Vol 1, pages TuC3-18-TuC3-25, 10-13 July 2000, Paris, France. Int. Soc. Information Fusion, Sunnyvale, CA, 2000.

[22] E. Binaghi, I. Gallo and M. Pepe. A neural adaptive model for feature extraction and recognition in high resolution remote sensing imagery. *Int. J. Remote Sensing*, 24(20): 3947-3959, 2003.

[23] M. Pesaresi. The remotely sensed city. Final report of the post-doctoral fellowship at the JRC, Ispra, Italy, 2000.

[24] B. Mannan, J. Roy, and K.A. Ray, "Fuzzy ARTMAP supervised classification of multi-spectral remotely-sensed images" *Intl. J. Remote Sensing*, Vol. 19, no. 4, pp. 767-774, 1998.

[25] I.L. Thomas, N.P. Ching, V.M. Benning, J.A. D'Aguanno. A review of multi-channel indices of class separability. *Int. J. Remote Sensing*, 8(5): 331-350, 1987.

[26] Q. Zhang, J. Wang, P. Gong, P. Shi. Study of urban spatial patterns from SPOT panchromatic imagery using textural analysis. *Int. J. Remote Sensing*, 24(21): 4137-4160, 2003.